Am J Physiol Cell Physiol 286: C372–C379, 2004.
First published October 15, 2003; 10.1152/ajpcell.00271.2003.

Role of cytoplasmic termini in sorting and shuttling of the aquaporin-2 water channel

Bas W. M. van Balkom,[1] Michael P. J. Graat,[1] M. van Raak,[1] Erik Hofman,[1] Peter van der Sluijs,[2] and Peter M. T. Deen[1]

[1]*Department of Cell Physiology, University Medical Center St. Radboud, Nijmegen Center for Molecular Life Sciences, Nijmegen, The Netherlands; and* [2]*Department of Cell Biology, Utrecht University, Utrecht, The Netherlands*

Submitted 29 June 2003; accepted in final form 12 October 2003

Van Balkom, Bas W. M., Michael P. J. Graat, M. van Raak, Erik Hofman, Peter van der Sluijs, and Peter M. T. Deen. Role of cytoplasmic termini in sorting and shuttling of the aquaporin-2 water channel. *Am J Physiol Cell Physiol* 286: C372–C379, 2004. First published October 15, 2003; 10.1152/ajpcell.00271.2003.—In mammals, the regulation of water homeostasis is mediated by the aquaporin-1 (AQP1) water channel, which localizes to the basolateral and apical membranes of the early nephron segment, and AQP2, which is translocated from intracellular vesicles to the apical membrane of collecting duct cells after vasopressin stimulation. Because a similar localization and regulation are observed in transfected Madin-Darby Canine Kidney (MDCK) cells, we investigated which segments of AQP2 are important for its routing to forskolin-sensitive vesicles and the apical membrane through analysis of AQP1-AQP2 chimeras. AQP1 with the entire COOH tail of AQP2 was constitutively localized in the apical membrane, whereas chimeras with shorter COOH tail segments of AQP2 were localized in the apical and basolateral membrane. AQP1 with the NH_2 tail of AQP2 was constitutively localized in both plasma membranes, whereas AQP1 with the NH_2 and COOH tail of AQP2 was sorted to intracellular vesicles and translocated to the apical membrane with forskolin. These data indicate that region N220-S229 is essential for localization of AQP2 in the apical membrane and that the NH_2 and COOH tail of AQP2 are essential for trafficking of AQP2 to intracellular vesicles and its shuttling to and from the apical membrane.

routing signals; chimera; Madin-Darby canine kidney cells; regulated trafficking

TO MAINTAIN WATER AND OSMOLYTE BALANCE, the human kidney daily forms 180 l of pro-urine. The main portion of the water from the pro-urine is reabsorbed, which occurs mainly through aquaporin-1 (AQP1) and AQP2 (9, 10, 35). AQP1, responsible for 90% of the water reabsorption, is constitutively present in the apical and basolateral membrane of proximal tubules and the descending limbs of Henle (40). The fine-tuning of water reabsorption takes place in the renal collecting duct and is regulated by the antidiuretic hormone arginine vasopressin (AVP). After release of AVP by the pituitary gland and binding to its type-2 receptor (V2R) in the basolateral membrane of collecting duct principal cells, an intracellular cAMP signaling cascade is initiated, resulting in the phosphorylation of AQP2 and its redistribution from vesicles to the apical membrane. Then, driven by an osmotic gradient, collecting duct water uptake and urine concentration is initiated via AQP2 in the apical and AQP3/AQP4 in the basolateral membranes (11, 37). Removal of AVP reverses this translocation process, restoring the water-impermeable state of the apical membrane (7, 23, 26). A proper regulation of AQP2 sorting and translocation to the apical membrane is thus of critical importance for human water homeostasis. At present, however, it is unclear which protein segments of AQP2 are critical for this regulation.

All AQPs are homotetrameric integral membrane proteins, consisting of subunits of about 30 kDa, which pass the membrane six times and have their NH_2 and COOH termini located in the cytosol. The membrane segments are connected by five loops, annotated A–E (shown in Fig. 1 for AQP1). Of the two intracellular loops of AQP2, the charged loop D only consists of about eight amino acids, whereas loop B is rather hydrophobic and will, based on resolved structure of AQP1 (31, 36), fold back into the membrane, forming part of the water pore. Although transmembrane domains (TMDs) cannot be excluded, this indicates that the cytosolic AQP2 NH_2 and COOH termini might be segments of importance in regulating AQP2 sorting and translocation. In fact, several studies have shown the importance of the AQP2 COOH tail in this. First, phosphorylation of Ser256 in the COOH tail is essential and sufficient for an apical membrane expression of AQP2 (13, 20, 22, 38). Second, AQP2 mutants encoded in congenital dominant nephrogenic diabetes insipidus (NDI), a disease characterized by the inability of the kidney to concentrate urine in response to AVP, are missorted to organelles such as the Golgi complex region and late endosomes/lysosomes because of mutations in the AQP2 COOH tail (21, 25, 27, 30).

Our studies on AQP2 have been performed in Madin-Darby canine kidney (MDCK) cells, which appear to be a good model system to study AQP2 trafficking and regulation. As in collecting ducts, AQP2 expressed in MDCK cells (wt10 cells) is localized in intracellular storage vesicles in nonstimulated cells and translocates to the apical membrane after stimulation by AVP or the adenylate cyclase activator, forskolin (7). Heterologous expression of AQP1 in these cells, however, leads to a random distribution of this protein over the apical and basolateral membranes, which is in line with its localization in proximal tubules and the descending limbs of Henle (6, 24). Such a distribution pattern has been found for several other membrane proteins and is generally been considered to result from bulk-flow transport of proteins lacking specific sorting signals (16). This indicates that the routing information of AQP2 is contained within the protein itself and can be studied in MDCK cells. In a subsequent study, chimeric proteins consisting of an AQP1 core and the COOH tail of AQP2

Address for reprint requests and other correspondence: P. M. T. Deen, 160, Dept. of Physiology, Research Tower, 7th Floor, UMC St. Radboud, PO Box 9101, 6500 HB Nijmegen, The Netherlands (E-mail: p.deen@ncmls.kun.nl).

The costs of publication of this article were defrayed in part by the payment of page charges. The article must therefore be hereby marked "*advertisement*" in accordance with 18 U.S.C. Section 1734 solely to indicate this fact.

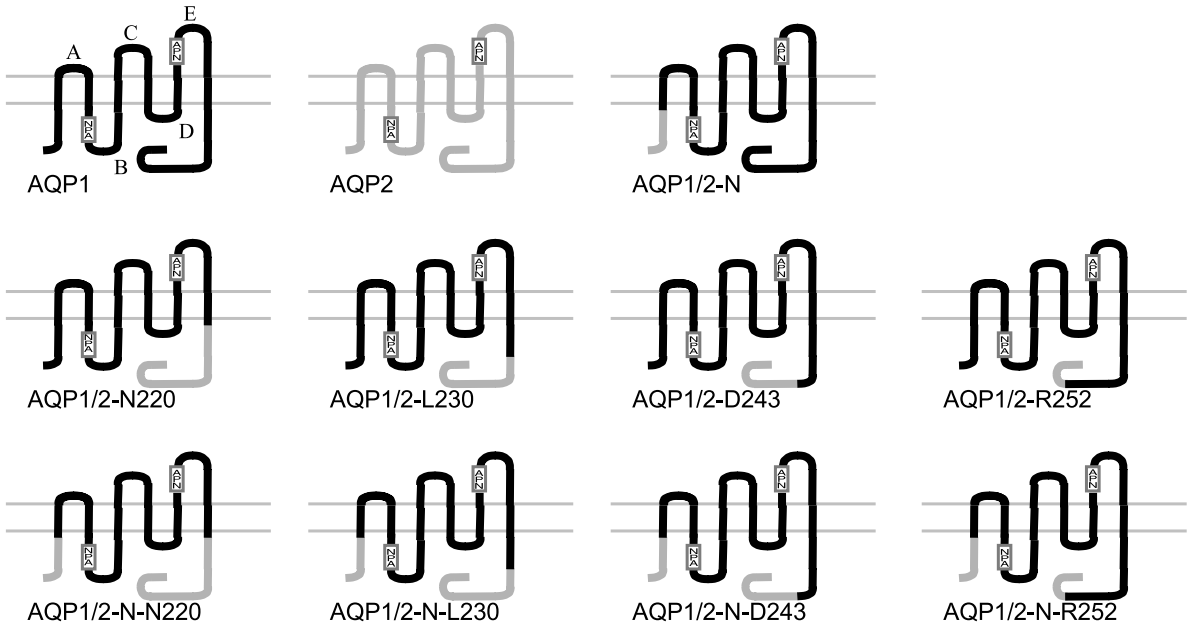

Fig. 1. Schematic overview of the used aquaporin-1 (AQP1)-AQP2 chimeras. Schematic representation of the different AQP1-AQP2 chimeras studied showing a simplified membrane topology and characteristic NPA boxes. Segments derived from AQP2 are indicated in gray and those from AQP1 in black. The annotations used throughout this study are indicated below each representation and are explained in the text.

localized in the apical membrane of MDCK cells, independent of forskolin stimulation, which indicates that the AQP2 COOH tail is important for its localization in the apical membrane but that it is not sufficient for trafficking to the intracellular storage vesicles (8).

Therefore, to further define which segments of AQP2 are relevant for its localization in the apical membrane and to intracellular storage vesicles, several AQP1/AQP2 fusion proteins were stably expressed in MDCK cells and analyzed in detail.

MATERIALS AND METHODS

Expression Constructs

Expression in MDCK cells. All constructs generated encoded AQP1-AQP2 chimeric proteins, in which parts of the NH_2 and/or COOH termini were exchanged. On the basis of the alignment of AQP1 and AQP2, segments of the AQP1 COOH tail have been exchanged for homologous segments of the AQP2 COOH tails. As such, chimeric proteins were made in which AQP1 ending at Y227, D237, V250, and D259 were followed by AQP2 COOH tail segments starting at N220, L230, D243, and R252, respectively (Fig. 1). These latter annotations were used in the corresponding expression constructs and chimeric proteins. All cDNAs were cloned into the pCB6 expression vector.

Except when indicated, all constructs were generated by three-point PCR reactions as described for AQP1/2-N220 (8). Constructs encoding AQP1 with different AQP2 COOH tails (AQP1/2-N220, -L230, -D243, -R252) were made as described for AQP1/2-N220 (8), except for the mutagenesis primers [5′-ccctggcagtgctgatctat**aactacgtgctgtttccgcc**-3′, 5′-tggccccacgcagcagcgac**ctgtcggagcgcctggcagt**-3′, 5′-tgtggaccagtggccaagtg**gacaccgattgggaggagcg**-3′ or 5′-atgacctggatgctgatgat**cgacggcggcagtcggtgga**-3′, respectively (AQP2 sequences in bold)]. To generate a construct coding for AQP1 with the NH_2 and COOH termini of AQP2 (AQP1/2-N-N220), an anti-sense primer, which fuses AQP2-E16 to AQP1-F18 (5′-aagagggtcatggccaggaactctgcgaacacagccctgg-3′) was used in a PCR reaction with a T7 RNA polymerase primer using pBS-AQP2 (10) as a template. This fragment was combined with the pCB6-AQP1/2-N220 construct (9), T7 RNA polymerase primer, and a reverse pCB6 primer (5′-gactggagtggcaacttcc-3′) in a second PCR reaction. After digestion with *Eco*RI, blunt-ending, and digestion with *Avr*II, the fragment was isolated and cloned into the *Avr*II and blunted *Sst*I site of pCB6-AQP1/2-N220. To generate a construct encoding the NH_2 tail of AQP2 fused to AQP1 (AQP1/2-N), an *Avr*II-*Hin*dIII fragment was digested from pBS-AQP1 (6) and ligated into an *Avr*II-*Hin*dIII-digested AQP1/2-N-N220, thereby replacing the COOH tail of AQP2 for the COOH tail of AQP1. To generate constructs encoding an AQP1 core region with the NH_2 tail and COOH tails of different lengths of AQP2, *Avr*II-*Xba*I fragments coding for AQP1/2-N-L230, AQP1/2-N-D243, or AQP1/2-N-R252 in pCB6 were cloned into the corresponding sites of pCB6-AQP1/2-N.

For expression of AQP1/2-N220 proteins in which three adjacent (triple) amino acids (N220-V222, L223-P225, P226-S229) in the region N220-S229 were changed into alanines (AQP1/2-N220trA1, -trA2, -trA3, respectively), three-point PCR reactions were performed with complementary forward and reverse mutagenesis primers [forward sequences: 5′-gtgctgatctat**gccgcggcgctgtttccgc**-3′, 5′-ctat**aactacgtggccgcggcgccagccaag**-3′, 5′-**gctgtttccggcagccgcggccctgtcggag**-3′, respectively (introduced mutations and restriction sites are underlined and italicized, respectively)], and pCB6 reverse (5′-cactggagtggcaacttcc-3′) and forward (5′-gggcggtaggcgtgtacg-3′) primers, using pCB6-AQP1/2-N220 as a template. The *Avr*II-*Hin*dIII fragments of the final PCR product were exchanged for the corresponding fragment in pCB6-AQP1/2-N220. For constructs encoding AQP2 in which W2, F9, F14, and N220-S229 were changed into alanines, complementary mutagenesis primers (forward primers 5′-ctgcagcatggcggaactccgctcc-3′ for W2A, 5′-tccatagccgccctccagggct-3′ for F9A, 5′-agggctgtggccgca*gaattc*c-3′ for F14A, 5′-cctcctctacgcctacgtgctg-3′ for N220A, 5′-cctctacaacgccgtgctgtttcc-3′ for Y221A, 5′-ctacaactacgcgctgtttccg-3′ for V222A, 5′-caactacgtggcgtttccgccag-3′ for L223A, 5′-ctacgtgctggctccgccagcc-3′ for F224A, 5′-cgtgctgtttgcgccagccaag-3′ for P225A, 5′-gctgtttccggcagccaagagc-3′ for P226A, 5′-ccgccagccgcgagcctgtcgg-3′ for K228A) were used in combination with T7 and Sp6 RNA polymerase primers, and pT7Ts-AQP2 (30) as

a template. Final PCR products were digested with *Bgl*II and *Spe*I and ligated into the *Bgl*II and *Xba*I sites of pCB6.

Expression in yeast. For expression of the COOH tail of AQP2 fused to the Gal4 activation domain in a LexA/Gal4 yeast two hybrid system (1), a standard PCR reaction was performed using an AQP2 forward (5′-gcat*ggatcc*tgtttccgccagcc-3′; *Bam*HI site in italic) and reverse (5′-gatc*ctcgag*gcggccctcaggccttgg-3′; *Xho*I site in italic) using pBS-AQP2 as a template. The obtained 170-bp PCR product was digested with *Bam*HI and *Xho*I and ligated into the corresponding sites of pACTII (BD Biosciences, Palo Alto, CA), thereby creating pACTII-AQP2C. With this cloning, the AQP2 tail starting at amino acid Phe224 was cloned in frame with the Gal4 protein. To make the construct coding for the LexA DNA binding domain coupled to the AQP2 COOH tail, a forward primer (5′-gatcg*gaattc*ccgccagccaa-gagcct-3′; *Eco*RI site in italic), the above-mentioned reverse primer, and pBS-AQP2 were combined in a PCR reaction, the product was cut with *Eco*RI and *Xho*I, and the isolated fragment was cloned into the same sites of pBTM116 (1), with which pBTM116-AQP2C was created. With this, an identical tail as for in pACTII-AQP2C was cloned in frame with the LexA protein.

To generate a construct coding for the NH_2 tail of AQP2 fused to the NH_2 terminus of the LexA DNA binding domain, a forward (5′-gatc*gaattc*cgcagggctctctgcag-3′; *Eco*RI site in italic) and reverse primer (5′-gatc*gtcgac*ctctgcgaacacagc-3′; *Sal*I site in italic) were used on a pBS-AQP2 template in a standard PCR reaction. After digestion with *Eco*RI and *Sal*I, the obtained PCR fragment of 74 bp was ligated into the corresponding sites of pFBL23 (3).

Introduction of only the desired mutations in all final constructs was confirmed by DNA sequence analysis of the cDNA inserts.

Cell Culturing, Transfection, and Immunocytochemistry of MDCK Cells

MDCK type I cells expressing rat AQP1 or human AQP2 were as described (6, 7). MDCK cells were grown in Dulbecco's modified Eagle's medium (DMEM) supplemented with 5% (vol/vol) fetal calf serum at 37°C in 5% CO_2. Stable transfectants were obtained and selected as described in detail (8). Representative stably transfected clones were selected in the following way: first, the obtained clones needed to have expression of the transfected protein, which was analyzed by immunoblotting, and a proper cuboidal morphology. In a second step of at least four independent clones, the intracellular localization of the expressed protein was determined by immunocytochemistry and confocal laser scanning microscopy (CLSM) as described (8). For this, cells were seeded at 1.5×10^5 cells/cm^2 on 1.13-cm^2 polycarbonate filters (Corning Costar Europe, Badhoevedorp, The Netherlands), grown for 2 days, and subsequently treated overnight with 5×10^{-5} M indomethacin to reduce basal intracellular cAMP levels. Cells were then incubated for 45 min with DMEM/indomethacin with or without 5×10^{-5} M forskolin, which activates adenylate cyclase. As primary antibodies, guinea pig or rabbit anti-AQP2 (5), mouse anti-Lamp2 (Ref. 32; kindly provided by A. Le-Bivic, Marseilles, France), or rabbit anti-protein disulfide isomerase (PDI; Ref. 34; kindly provided by W. Hendriks, Nijmegen, The Netherlands) were used, whereas Alexa 488- and Alexa 594-conjugated anti-rabbit and anti-mouse antibodies (Molecular Probes, Leiden, The Netherlands) were used as secondary probes, respectively. For Lamp2 detection, filters were incubated in PBS containing 50 mM NH_4Cl for 10 min after fixation, washed three times with PBS, and blocked with PBS containing 0.1% BSA for 20 min. Filters were then washed three times with PBS, after which they were incubated in PBS containing 0.05% saponin and the 1:100 diluted primary antibodies for at least 30 min. Filters were next washed three times with PBS, incubated with secondary antibody, 1:100-diluted in PBS for 30 min, and washed with PBS. After the last wash, filters were mounted and analyzed as described (8). Of a subcellular localization pattern that was consistent for at least three out of the four clones, one or two of these clones were selected as representative clones for further studies.

Side-Specific Biotinylation and Immunoblotting

MDCK cells were seeded at 1.5×10^5 cells/cm^2 on 9.6-cm^2 polycarbonate filters (Corning Costar Europe) and grown and treated as described above. Next, proteins present in the apical membrane were subjected to a biotinylation assay as described (2) and analyzed by immunoblotting. For immunoblotting, protein samples were denatured by incubation for 30 min at 37°C in 1× Laemmli buffer, subjected to electrophoresis on a 13% SDS-polyacrylamide gel (Fluka Biochimica, Switzerland), and blotted onto polyvinylidene fluoride (PVDF) membranes (Millipore, Bedford, MA). After being blocked in 5% nonfat dried milk (NFDM) in TBS-T (20 mM Tris·HCl, 73 mM NaCl, 0.2% Tween 20, pH 7.6) for 1 h, membranes were incubated with 1:3,000 diluted affinity-purified rabbit anti-AQP2 antibodies [raised against the 15 COOH-terminal amino acids of rat AQP2 (5)], 1:100 diluted mouse monoclonal AQP1 antibodies (17), or 1:1,000 diluted rabbit anti-LexA antibodies (provided by W. Hendriks). Dilutions were made in TBS-T with 1% NFDM. As secondary antibodies, goat anti-rabbit or goat anti-mouse antibodies coupled to horseradish peroxidase (Sigma, St. Louis, MO), which were diluted 1:5,000 or 1:2,000 in TBS-T, respectively, were used. Antibody-bound proteins were visualized using enhanced chemiluminescence (Pierce, Rockford, IL).

Yeast Two Hybrid Analysis

For cotransformation of bait and prey constructs, a 20-ml overnight culture of L40 yeast cells in 1% yeast extract, 2% peptone, 2% dextrose, and 200 mg/l adenine (YPDA) medium was used to inoculate 100 ml of YPDA to 0.2 A_{600}. At an A_{600} of 0.8, the cells were collected by centrifugation at 4,200 *g* at 4°C for 15 min and washed with 400 ml of sterile distilled H_2O. Then, cells were pelleted, washed in 160 ml H_2O, pelleted at 1,300 *g* (10 min, 4°C), and transfected according to Gietz and Schiestl (14) using 1 μg of bait and prey plasmids. After incubation at 30°C for 30 min and heat shock at 42°C for 30 min, cells were harvested by centrifugation at 1,900 *g* for 3 min, washed with distilled H_2O, resuspended in 50 μl of distilled H_2O, and plated on SD-Trp-Leu plates. If bait and prey proteins interact, β-galactosidase is produced, which will give a blue-colored colony when incubated with the β-galactosidase substrate X-gal. Therefore, after 3–4 days, colonies were tested for β-galactosidase expression by a colony lift assay (4). For this, colonies were transferred onto 3MM Whatmann filters, permeabilized in liquid N_2, and overlaid with 0.2 mg/ml X-Gal in TBSY (150 mM NaCl, 50 mM Tris·HCl, pH 7.4, and 0.8% agarose). As a positive control on interaction, L40 cells were transformed with pBTM116 and pACTII constructs encoding the COOH tail of rat $NaPO_4$ cotransporter (NaP_i-IIa) and Hsp84, respectively, which have been reported to interact (15). As negative controls, yeast cells were transfected with the AQP2 NH_2 or COOH tail plasmids combined with an empty bait or prey plasmid.

Image Quantification Analysis

To create an objective index for basolateral vs. apical expression of the AQP proteins, the integrated optical density (IOD) of equal basolateral or apical membrane segments within a fixed square area was determined using Image-Pro Plus analysis software (Media Cybernetics, Silver Spring, MD). Background IOD values, determined within the nuclear area of the particular cell, were subtracted from the obtained basolateral and apical IOD values. The B/A sorting index is defined as the IOD of the basolateral membrane segment divided by the IOD of the apical membrane segment. Of eight independent cells of representative images and three segments of the basolateral and apical membrane per cell, the mean B/A sorting index ± SE was determined. The significance of a change in sorting index between two experimental settings was determined with an independent two population *t*-test.

RESULTS

Determination of the Apical Targeting Segment in the AQP2 COOH Terminus

In the used annotations for the chimeric proteins (e.g., AQP1/2-N-N220), the core region (i.e., TMD 1 through 6) is always of AQP1. The parts of AQP2 replacing homologous parts of AQP1 are indicated after the hyphen. After the hyphen, N indicates the AQP2 NH_2 terminus, while N220, L230, D243, and R252 indicate the starting amino acid of AQP2 COOH tail present in the chimera. (see also Fig. 1). Recently, we have shown that AQP1/2-N220 is sorted to the apical membrane, independent of forskolin treatment (8). This indicated that the COOH tail of AQP2 is necessary for apical localization of AQP2. To further define the region that is crucial for its apical targeting, we investigated the intracellular localization of an additional set of chimeras, namely AQP1/2-L230, AQP1/2-D243, and AQP1/2-R252, consisting of AQP1 in which the COOH tail was exchanged with corresponding but decreasing parts of the AQP2 COOH tail (Fig. 1). MDCK cell clones stably expressing these chimeras were selected, treated with or without forskolin, and subjected to immunocytochemistry. CLSM analysis revealed that AQP1/2-L230, AQP1/2-D243, and AQP1/2-R252 were strongly expressed in the basolateral membrane and, to a lesser extent, in the apical membrane (Fig. 2). As reported (8) and in contrast to the chimeras above, AQP1/2-N220 was mainly localized in the apical membrane. Similar to AQP1/2-N220, forskolin did not appear to change the subcellular localization of AQP1/2-L230, AQP1/2-D243, or AQP1/2-R252. As reported (6, 7), forskolin treatment did not change the basolateral and apical membrane localization of AQP1, although it did cause a translocation of AQP2 from intracellular vesicles to the apical membrane (Fig. 4*A*). Quantitative analysis of the ratio of basolateral vs. apical membrane expression revealed a B/A sorting index (mean ± SE) for AQP1/2-N220 of 0.18 ± 0.1, while AQP1, AQP1/2-L230, AQP1/2-D243, and AQP1/2-R252 showed B/A sorting indexes of 0.70 ± 0.1, 0.78 ± 0.2, 0.92 ± 0.2, and 0.90 ± 0.1 (for each, $n = 8$), respectively. Statistical analysis of these B/A sorting indexes revealed that the localization of AQP1/2-N220 differed significantly from those of AQP1, AQP1/2-L230, AQP1/2-D243, and AQP1/2-R252 ($P < 0.001$), although the subcellular localization of the latter four did not significantly differ.

N220-S229 Segment in AQP1/2 Proteins Is Highly Sensitive to Mutations

The N220-S229 segment of AQP2 consists of the amino acids **NYVL**FPPAKS, of which the bold amino acids are part of the sixth TMD. To further pinpoint the amino acids important for the apical trafficking of AQP2, we performed a triple alanine scan in which the amino stretches N_{220}YV (AQP1/2-N220-trplA1), L_{223}FP (AQP1/2-N220-trplA2), and P_{226}AKS (AQP1/2-N220-trplA3) were changed into alanines. After transfection of MDCK cells, most G418-resistant clones revealed no AQP signal with immunoblotting. A few clones of each transfection, however, showed AQP2-specific bands of ~16, 29, 32, 35, 38, and 40 kDa, but only after long exposure times (Fig. 3*A3*). As anticipated, immunocytochemical analysis of these few AQP2-positive cell lines showed a weak, spotlike, and dispersed staining throughout the cell (exemplified in Fig. 3*A2*). These data indicate that these AQP1/2 proteins were unstable. Therefore, we decided to change each amino acid within the N220-S229 region of AQP2 into alanine. Subsequent analyses revealed immunoblot signals (29- and 40- to 45-kDa bands) and cellular distribution patterns (redistributed with forskolin from intracellular vesicles to the apical membrane) for AQP2 proteins with V222A, P225A, K228A, or S229A mutations that were similar to those of wt-AQP2 (Fig. 3*B*). In contrast, AQP2 proteins with N220A, Y221A, L223A, F224A, or P226A mutations revealed an ER-retained expression pattern (29- and 32-kDa proteins), which was immunocytochemically confirmed by their colocalization with the ER marker protein PDI (Fig. 3*C*).

Role of the AQP2 NH_2 Tail in Trafficking to Forskolin-Sensitive Intracellular Vesicles

Our results above revealed that the COOH tail of AQP2 was not sufficient to sort the AQP1/2 chimeras to intracellular vesicles in nonstimulated cells. To investigate whether such

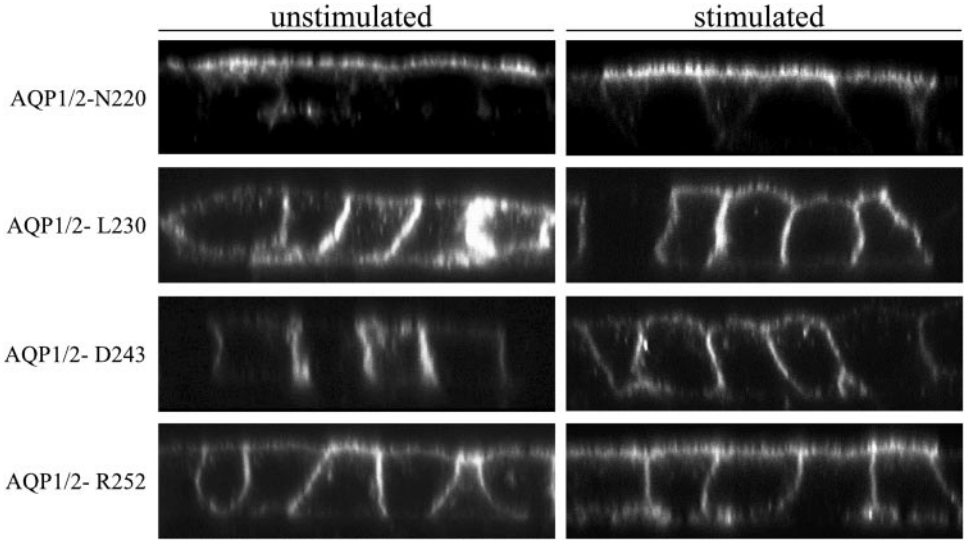

Fig. 2. Subcellular localization of AQP1/2 chimeras with different AQP1/2 COOH tail segments. MDCK cells expressing AQP1/2 chimeric proteins with different AQP1/2 COOH termini (indicated at *left*) were grown to confluence and incubated overnight with indomethacin to reduce basal cAMP levels. Cells were then incubated with indomethacin in the absence (unstimulated) or presence (stimulated) of forskolin and subjected to immunocytochemistry. Independent of forskolin stimulation, AQP1/2-N220 was expressed in the apical membrane, while AQP1/2-L230, -D243, and -R252 were expressed in the apical and basolateral membranes.

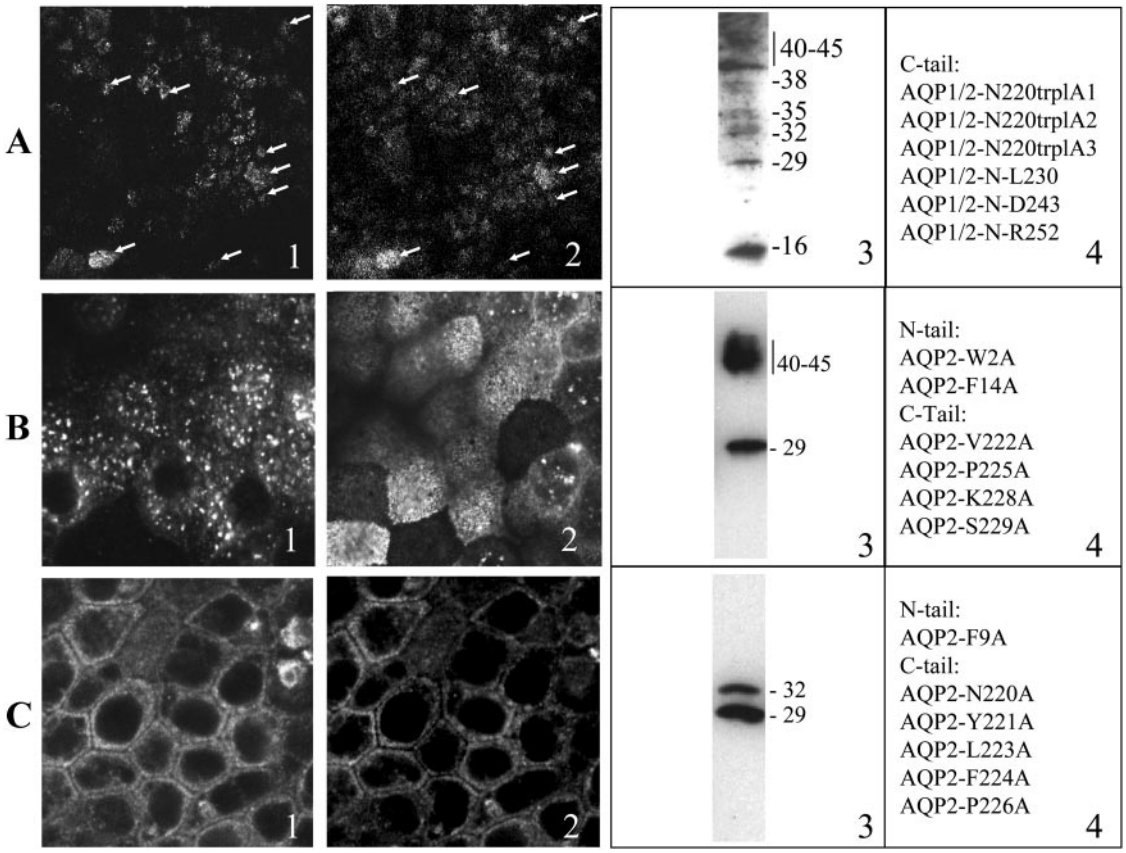

Fig. 3. Immunocytochemical and immunoblot data of alanine scan mutants of the NH$_2$ and COOH tail of AQP2 and AQP1/2 chimeras. With the analyses of AQP1/2 chimeras and alanine scan mutants in the NH$_2$ and COOH tail of AQP2 (see text), 3 different cellular phenotypes were observed. In phenotype *A*, the mutants were weakly expressed, showed a dotlike staining throughout the cell (*A1*), colocalized with the late-endosome/lysosomal marker protein Lamp2 (*A2*, arrows), and were detected as 16-, 29-, 32-, 35-, 38-, and 40-kDa and higher bands on immunoblots (*A3*). In phenotype *B*, mutants were like wt-AQP2 and were stored in vesicles without stimulation (*B1*), were translocated to the apical membrane with forskolin stimulation (*B2*), and were detected as nonglycosylated 29-kDa and complex-glycosylated 40- to 45-kDa proteins on immunoblot (*B3*). In phenotype *C*, the mutants were retained in the ER (*C1*), colocalized with the ER marker protein PDI (*C2*), and detected as 29- and 32-kDa high-mannose glycosylated proteins on immunoblot (*C3*). *A4*, *B4*, and *C4* denote the mutants that showed a cellular phenotype represented by the particular panel. Images shown are from AQP1/2-N-R252 (*A*), wt-AQP2 (*B*), or AQP2-F9A (*C*).

information is contained within the NH$_2$-terminal tail of AQP2, constructs were made coding for AQP1/2-N, which is AQP1 with the NH$_2$ tail of AQP2, and AQP1/2-N-N220, which is AQP1 with both the NH$_2$ and COOH tails of AQP2 (Fig. 1). CLSM analysis of stable clones revealed that AQP1/2-N was, independent of forskolin treatment, localized in the basolateral and apical membrane with a B/A sorting index of 0.65 ± 0.27 (n = 8) (Fig. 4*A*). This index was not significantly different from those of AQP1 and the chimeras AQP1/2-L230 to AQP1/2-R252. In contrast, AQP1/2-N-N220 was localized in intracellular vesicles and was mainly redistributed to the apical membrane with forskolin. Its B/A sorting index was 0.23 ± 0.05 (n = 8).

To confirm their localization in the apical membrane and the extent of increase of their expression in this membrane with forskolin, these chimeras and controls were subjected to apical cell surface biotinylation assays. In line with the immunocytochemical results, immunoblotting for biotinylated AQP proteins revealed that AQP1/2-N and AQP1 were expressed at similar levels in the apical membrane with or without forskolin, whereas AQP1/2-N-N220 and AQP2 expression in the apical membrane was increased upon treatment with forskolin (Fig. 4*B*). Densitometric analysis of the blot signals revealed that forskolin induced a 1.0- (24.81 ± 0.4 to 24.5 ± 0.7; densities in arbitrary units), 1.3- (20.61 ± 0.4 to 26.88 ± 0.09), 6.1- (3.23 ± 1.0 to 19.70 ± 1.5), and 7.3-fold (2.60 ± 0.5 to 18.97 ± 2.1) increase in apical membrane expression for AQP1/2-N, AQP1, AQP1/2-N-N220, and AQP2, respectively. These data indicated that the NH$_2$ tail of AQP2 was essential for the trafficking of AQP2 to forskolin-sensitive storage vesicles.

Which Segment of the AQP2 COOH Tail Is Involved in Trafficking to Intracellular Vesicles?

The plasma membrane localization of AQP1/2-N and AQP1/2-N220 and vesicular localization of AQP1/2-N-N220 indicated that both the NH$_2$ and COOH termini of AQP2 were needed for sorting of the AQP1/2-N-N220 chimera to intracellular vesicles. To investigate which part of the AQP2 COOH terminus was important in this, we exchanged the COOH tail of AQP1/2-N-N220 for the COOH tails of AQP1/2-L230, -D243, or -R252, resulting in constructs encoding AQP1/2-N-L230, -D243, and -R252, respectively. Immunoblot analysis of

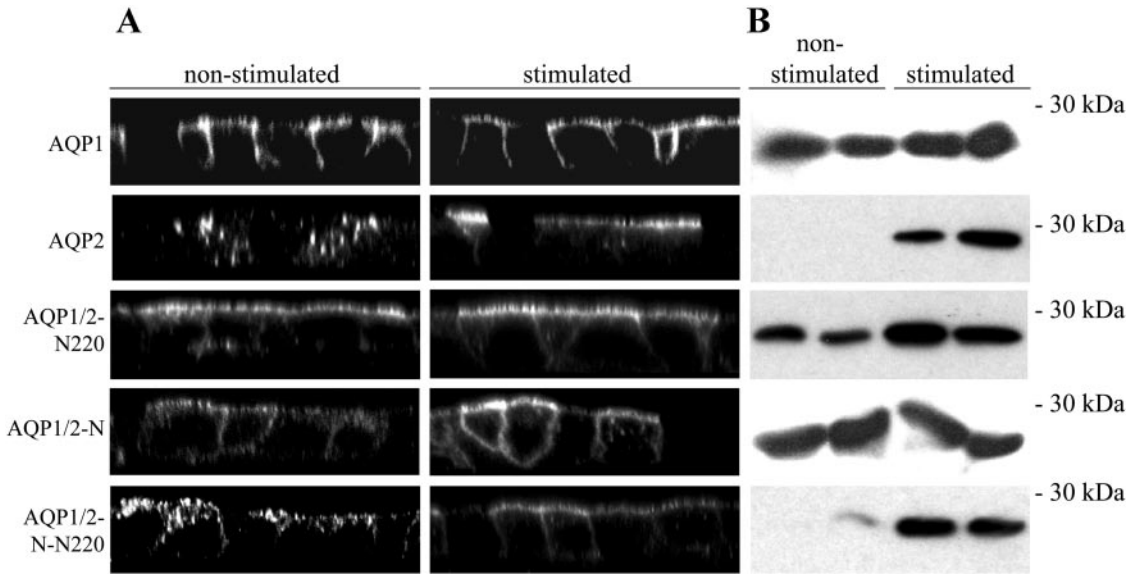

Fig. 4. Subcellular localization of AQP1/2 chimeras or AQP2 with NH_2 tail modifications. MDCK cells expressing AQP1, AQP2, and AQP1 with an AQP2 NH_2 tail (AQP/1/2-N) or AQP1 with an AQP2 NH_2 and COOH tail (AQP1/2/-N-N220) were grown, treated, and subjected to assays as described in the legend of Fig. 2. *A*: *X-Z* confocal images of MDCK cells expressing the different AQP proteins. Independent of forskolin stimulation, AQP1 and AQP1/2-N were expressed in the apical and basolateral membrane. In contrast, forskolin shifted the localization of AQP1/2-N-N220 and wt-AQP2 from intracellular vesicles to the apical membrane. *B*: apical membrane expression of the different AQP proteins. Cells were subjected to apical cell surface biotinylation. AQP1 and AQP1/2-N220 were already expressed in the apical membrane, and forskolin induced their apical membrane expression 1.3- and 1.0-fold, respectively. In contrast, apical membrane expression of AQP2 and AQP1/2-N-N220 was low in nonstimulated cells and was increased more than 6.0-fold upon treatment with forskolin.

numerous clones, however, showed expression levels and a subcellular localizations as found for the triple alanine scan mutants described above (Fig. 3*A*). The low expression levels, the detection of a 16-kDa degradation product, and the difference from a typical ER-retained AQP2 expression pattern suggested that these proteins were degraded by the lysosomal degradation pathway. To test for this, two AQP1/2-N-R252 clones were subjected to colocalization studies with the late endosomal/lysosomal marker protein Lamp2 or the Golgi marker protein 58K. CLSM analysis revealed a weak punctate AQP-specific expression pattern, which partially costained for Lamp2 (Fig. 3*A2*) and not for 58K (not shown).

Analysis of a Possible Interaction Between the AQP2 NH_2 and COOH Tails

AQPs are expressed as homotetramers (25, 38, 45, 47). On the basis of the recently resolved AQP1 structure (36), which does not cover the tails, it can be deduced that the distance between the NH_2 and COOH termini of an AQP1 monomer is about 25 Å, whereas that between the NH_2 and COOH termini of neighboring monomers is 12–15 Å, indicating that about 12 or 8 amino acids are needed to cross the distance, respectively. Because the NH_2 (16 amino acids) and COOH termini (46 amino acids) of AQP2 are large enough to cross these intra- and intermolecular distances, both the NH_2 and COOH tails of AQP2 appeared to be required for trafficking of AQP1/2 proteins to intracellular vesicles, and interactions between NH_2 and COOH termini have shown to be important for the regulation of several proteins (12, 18, 19), we investigated whether the NH_2 and COOH tails of AQP2 could physically interact with each other using yeast two hybrid assays. As negative controls, L40 cells were transformed with AQP2 COOH tail or NH_2 tail constructs combined with empty bait or prey vectors. After growth on medium selective for transformed cells, ~200–300 colonies of each plate were screened for interaction. As shown in Fig. 5, no interaction could be demonstrated between the NH_2 and COOH termini of AQP2. As anticipated, the negative controls neither showed any staining, whereas the positive control clearly turned blue. In addition, immunoblotting for the bait and prey proteins revealed that the tested yeast cells did express the respective AQP2 NH_2 tail and COOH tail fusion proteins (not shown).

DISCUSSION

Region N220-S229 of AQP2 Seems Crucial for Its Apical Localization

Recently, we showed that the AQP2 COOH tail starting at N220 was necessary for AQP2 sorting to the apical membrane. To determine which part of the AQP2 COOH tail is important in this, we analyzed the expression of AQP1/2-L230, AQP1/2-D243, and AQP1/2-R252 in MDCK cells. Immunocytochemical and biotinylation analyses revealed that, in contrast to AQP1/2-N220 and wt-AQP2, all these chimeric proteins were distributed as found for AQP1, because all three chimeras and AQP1 were sorted to a similar extent to the apical and basolateral membranes (Fig. 2). Region N220-S229 is present in AQP1/2-N220 and AQP2 but is lacking from the other AQP1/2 chimeras and AQP1. As suggested for carboxypeptidase M (29), the observed distribution patterns could be the result of the removal of a (weak) basolateral sorting signal in the proximal region of the AQP1 COOH tail. However, because the random plasma membrane distribution pattern of AQP1 in MDCK cells is similar to that found for bulk-flow membrane

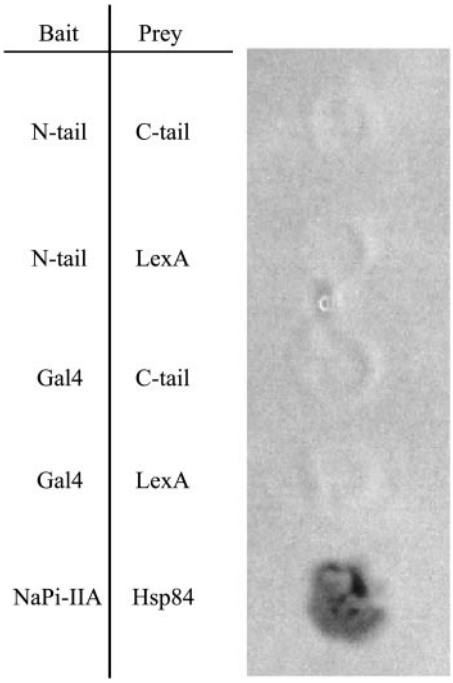

Fig. 5. Analysis of direct interaction between the AQP2 NH_2 and COOH tails. A Gal4-AQP2 NH_2 tail bait and a LexA-AQP2 COOH tail prey construct (both indicated) were expressed in L40 yeast cells. As negative controls, empty bait (Gal4) and prey (LexA) constructs were cotransfected with the above-mentioned prey and bait constructs, respectively. As a positive control (15), Gal4 fused to the COOH tail of the Na/P_i IIa cotransporter and LexA fused to mouse Hsp84 was taken along. Analysis of the β-galactosidase expression, which is indicative of the expression of interacting proteins, revealed no interaction between the NH_2- and the COOH-terminal tails of AQP2, in contrast to the positive control.

proteins, which are thought to lack sorting signals (16), we favor the thought that region N220-S229 of the AQP2 tail contains information responsible for the apical targeting of AQP2. If the N220-S229 region is relevant, it remains at present unclear which motif in the N220-S229 segment is responsible for the apical localization of AQP2, because further mutations in this region resulted in wt-AQP2 or ER-retained expression patterns.

AQP2 NH_2 and COOH Termini Are Essential and Sufficient for Trafficking to Forskolin-Sensitive Vesicles and Translocation to the Apical Membrane

AQP1/2-N showed a basolateral and apical membrane expression with or without forskolin, indicating that the NH_2 tail of AQP2 is not sufficient for sorting to intracellular vesicles. AQP1/2-N-N220, however, was localized in forskolin-sensitive vesicles and was mainly targeted to the apical membrane with forskolin (Fig. 4). Because AQP1/2-N220 was present in the apical membrane with or without forskolin stimulation (Fig. 2), this indicated that the NH_2 and COOH termini of AQP2 are both necessary and sufficient to sort AQP2 to intracellular vesicles and to fully confer the cAMP-dependent shuttling from intracellular vesicles to the apical membrane, as observed for wt-AQP2. In line with this, forskolin increased the apical membrane expression of AQP1/2-N-N220 and wt-AQP2 more than sixfold, whereas the forskolin-induced increase in apical membrane expression of AQP1 and AQP1/2-N220 was less than 1.5-fold (Figs. 2 and 4). Because wt-AQP2 and AQP1/2-N-N220 did not colocalize with several vesicular marker proteins, it is at present unclear whether wt-AQP2 and AQP1/2-N-N220 are localized to the same intracellular vesicles. However, the significantly higher B/A sorting index for forskolin-stimulated AQP1/2-N-N220 compared with wt-AQP2 indicates that at least a small portion of AQP1/2-N-N220 is sorted to different vesicles.

For K^+ channels, the NH_2 and COOH termini appear to make direct interactions (18, 19), whereas other channels are regulated by proteins interacting with the NH_2 and COOH termini. AQPs are expressed as homotetramers (21, 33, 39, 41). Our yeast two-hybrid assays revealed no interaction between the NH_2 and COOH termini of AQP2 (Fig. 5), which indicates that unless putatively formed NH_2 tail/COOH tail complexes were not able to pass the nuclear membrane, the AQP2 NH_2 and COOH tails do not directly interact with each other. It remains to be determined whether AQP2 is regulated by interacting protein, because no AQP2 interacting proteins has been identified yet.

The AQP2 NH_2 Terminus Makes Chimeras Prone to Degradation

From our experiments, the high instability of AQP1/2-N-L230, -D243, -R252 compared with the other studied AQP1/2 proteins is striking. Several results obtained suggest that these chimeras were targeted for lysosomal instead of the endoplasmic reticulum-associated degradation (ERAD). First, the AQP-specific bands detected on blot (16, 29, 32, 35, 38, and 40 kDa) are different from those always observed for ER-retained mutants (29 and 32 kDa) (Fig. 3*C*; Refs. 5 and 28). Second, for G418-resistant clones expressing AQP1/2-N-L230, -D243, or R252, a similar punctate AQP distribution pattern was observed. Third, in colocalization experiments with two clones expressing AQP1/2-N-R252, these AQP signals colocalized partially with the late endosomal/lysosomal marker protein Lamp2 (Fig. 3*A*).

Compared to the stable AQP1/2-L230, D243, and R252 chimeras, these unstable chimeras only differ in that they have an AQP2 NH_2 tail instead of an AQP1 NH_2 tail. Because the AQP1/2-L230, -D243, and -R252 chimeras are expressed in the plasma membrane (Fig. 2) and the NH_2 tail of AQP2 but not of AQP1 appears to be important for sorting to intracellular vesicles (see above), these data might suggest that vesicular sorting and/or retrieval from the apical membrane is mediated by the AQP2 NH_2 tail and contributes to targeting these AQP proteins for degradation.

In summary, our data indicate that region N220-S229, which is the proximal region of the COOH terminus of AQP2, is of importance for sorting of AQP2 to the apical membrane and that the AQP2 NH_2 and COOH termini are essential and sufficient for sorting to forskolin-sensitive storage vesicles. Within the NH_2-and COOH-terminal regions, W2, F14, V222, P225, K228, and S229 are not essential for sorting to the apical membrane, nor to forskolin-sensitive vesicles. Further studies are needed to establish which amino acids in these segments are relevant for apical localization and trafficking to storage vesicles of AQP2 and through which mechanism this is accomplished.

ACKNOWLEDGMENTS

We are indebted to Drs. A. LeBivic, Marseille, France, and W. Hendriks, Nijmegen, The Netherlands, for gifts of anti-Lamp2 and anti-BiP/LexA antibodies, respectively, and we thank Jitske Stalpers for technical assistance.

GRANTS

This study was supported by grants from the Dutch Organization of Scientific Research (NWO-MW 902-18-292) (to P. M. T. Deen and P. van der Sluijs) and the European Union (QLK3-CT-2001-00987, QLRT-2000-00778) (to P. M. T. Deen).

REFERENCES

1. **Bartel PL and Fields S.** Analyzing protein-protein interactions using two-hybrid system. *Methods Enzymol* 254: 241–263, 1995.
2. **Baumgarten R, Van De Pol MH, Wetzels JF, van Os CH, and Deen PMT.** Glycosylation is not essential for vasopressin-dependent routing of aquaporin-2 in transfected Madin-Darby canine kidney cells. *J Am Soc Nephrol* 9: 1553–1559, 1998.
3. **Beranger F, Aresta S, de Gunzburg J, and Camonis J.** Getting more from the two-hybrid system: N-terminal fusions to LexA are efficient and sensitive baits for two-hybrid studies. *Nucleic Acids Res* 25: 2035–2036, 1997.
4. **Dalton S and Treisman R.** Characterization of SAP-1, a protein recruited by serum response factor to the c-fos serum response element. *Cell* 68: 597–612, 1992.
5. **Deen PMT, Croes H, van Aubel RA, Ginsel LA, and van Os CH.** Water channels encoded by mutant aquaporin-2 genes in nephrogenic diabetes insipidus are impaired in their cellular routing. *J Clin Invest* 95: 2291–2296, 1995.
6. **Deen PMT, Nielsen S, Bindels RJM, and van Os CH.** Apical and basolateral expression of aquaporin-1 in transfected MDCK and LLC-PK cells and functional evaluation of their transcellular osmotic water permeabilities. *Pflügers Arch* 433: 780–787, 1997.
7. **Deen PMT, Rijss JPL, Mulders SM, Errington RJ, van Baal J, and van Os CH.** Aquaporin-2 transfection of Madin-Darby canine kidney cells reconstitutes vasopressin-regulated transcellular osmotic water transport. *J Am Soc Nephrol* 8: 1493–1501, 1997.
8. **Deen PMT, Van Balkom BWM, Savelkoul PJ, Kamsteeg EJ, Van Raak M, Jennings ML, Muth TR, Rajendran V, and Caplan MJ.** Aquaporin-2: COOH terminus is necessary but not sufficient for routing to the apical membrane. *Am J Physiol Renal Physiol* 282: F330–F340, 2002.
9. **Deen PMT and van Os CH.** Epithelial aquaporins. *Curr Opin Cell Biol* 10: 435–442, 1998.
10. **Deen PMT, Verdijk MAJ, Knoers NVAM, Wieringa B, Monnens LAH, van Os CH, and van Oost BA.** Requirement of human renal water channel aquaporin-2 for vasopressin-dependent concentration of urine. *Science* 264: 92–95, 1994.
11. **Ecelbarger CA, Terris J, Frindt G, Echevarria M, Marples D, Nielsen S, and Knepper MA.** Aquaporin-3 water channel localization and regulation in rat kidney. *Am J Physiol Renal Physiol* 269: F663–F672, 1995.
12. **Endo S, Yamamoto Y, Sugawara T, Nishimura O, and Fujino M.** The additional methionine residue at the N-terminus of bacterially expressed human interleukin-2 affects the interaction between the N- and C-termini. *Biochem J* 40: 914–919, 2001.
13. **Fushimi K, Sasaki S, and Marumo F.** Phosphorylation of serine 256 is required for cAMP-dependent regulatory exocytosis of the aquaporin-2 water channel. *J Biol Chem* 272: 14800–14804, 1997.
14. **Gietz RD, Schiestl RH, Willems AR, and Woods RA.** Studies on the transformation of intact yeast cells by the LiAc/SS-DNA/PEG procedure. *Yeast* 11: 355–360, 1995.
15. **Gisler SM, Stagljar I, Traebert M, Bacic D, Biber J, and Murer H.** Interaction of the type IIa Na/P_i cotransporter with PDZ proteins. *J Biol Chem* 276: 9206–9213, 2001.
16. **Harter C and Wieland F.** The secretory pathway: mechanisms of protein sorting and transport. *Biochim Biophys Acta* 1286: 75–93, 1996.
17. **Jennings ML.** Monoclonal antibody against red blood cell CHIP28 protein (Abstract). *J Gen Physiol* 100: 21A, 1992.
18. **Jones PA, Tucker SJ, and Ashcroft FM.** Multiple sites of interaction between the intracellular domains of an inwardly rectifying potassium channel, Kir6.2. *FEBS Lett* 508: 85–89, 2001.
19. **Ju M, Stevens L, Leadbitter E, and Wray D.** The roles of N- and C-terminal determinants in the activation of the Kv2.1 potassium channel. *J Biol Chem* 278: 12769–12778, 2003.
20. **Kamsteeg EJ, Heijnen I, van Os CH, and Deen PMT.** The subcellular localization of an aquaporin-2 tetramer depends on the stoichiometry of phosphorylated and nonphosphorylated monomers. *J Cell Biol* 151: 919–930, 2000.
21. **Kamsteeg EJ, Wormhoudt TA, Rijss JPL, van Os CH, and Deen PMT.** An impaired routing of wild-type aquaporin-2 after tetramerization with an aquaporin-2 mutant explains dominant nephrogenic diabetes insipidus. *EMBO J* 18: 2394–2400, 1999.
22. **Katsura T, Gustafson CE, Ausiello DA, and Brown D.** Protein kinase A phosphorylation is involved in regulated exocytosis of aquaporin-2 in transfected LLC-PK1 cells. *Am J Physiol Renal Physiol* 272: F817–F822, 1997.
23. **Katsura T, Verbavatz JM, Farinas J, Ma T, Ausiello DA, Verkman AS, and Brown D.** Constitutive and regulated membrane expression of aquaporin 1 and aquaporin 2 water channels in stably transfected LLC-PK1 epithelial cells. *Proc Natl Acad Sci USA* 92: 7212–7216, 1995.
24. **King LS and Agre P.** Pathophysiology of the aquaporin water channels. *Annu Rev Physiol* 58: 619–648, 1996.
25. **Kuwahara M, Iwai K, Ooeda T, Igarashi T, Ogawa E, Katsushima Y, Shinbo I, Uchida S, Terada Y, Arthus MF, Lonergan M, Fujiwara TM, Bichet DG, Marumo F, and Sasaki S.** Three families with autosomal dominant nephrogenic diabetes insipidus caused by aquaporin-2 mutations in the C-terminus. *Am J Hum Genet* 69: 738–748, 2001.
26. **Marples D, Knepper MA, Christensen EI, and Nielsen S.** Redistribution of aquaporin-2 water channels induced by vasopressin in rat kidney inner medullary collecting duct. *Am J Physiol Cell Physiol* 269: C655–C664, 1995.
27. **Marr N, Bichet DG, Lonergan M, Arthus MF, Jeck N, Seyberth HW, Rosenthal W, van Os CH, Oksche A, and Deen PMT.** Heteroligomerization of an aquaporin-2 mutant with wild-type aquaporin- 2 and their misrouting to late endosomes/lysosomes explains dominant nephrogenic diabetes insipidus. *Hum Mol Genet* 11: 779–789, 2002.
28. **Marr N, Kamsteeg EJ, Van Raak M, van Os CH, and Deen PMT.** Functionality of aquaporin-2 missense mutants in recessive nephrogenic diabetes insipidus. *Pflügers Arch* 442: 73–77, 2001.
29. **McGwire GB, Becker RP, and Skidgel RA.** Carboxypeptidase M, a glycosylphosphatidylinositol-anchored protein, is localized on both the apical and basolateral domains of polarized Madin-Darby canine kidney cells. *J Biol Chem* 274: 31632–31640, 1999.
30. **Mulders SM, Bichet DG, Rijss JPL, Kamsteeg EJ, Arthus MF, Lonergan M, Fujiwara M, Morgan K, Leijendekker R, van der Sluijs P, van Os CH, and Deen PMT.** An aquaporin-2 water channel mutant which causes autosomal dominant nephrogenic diabetes insipidus is retained in the Golgi complex. *J Clin Invest* 102: 57–66, 1998.
31. **Murata K, Mitsuoka K, Hirai T, Walz T, Agre P, Heymann JB, Engel A, and Fujiyoshi Y.** Structural determinants of water permeation through aquaporin-1. *Nature* 407: 599–605, 2000.
32. **Nabi IR, Le Bivic A, Fambrough D, and Rodriguez-Boulan E.** An endogenous MDCK lysosomal membrane glycoprotein is targeted basolaterally before delivery to lysosomes. *J Cell Biol* 115: 1573–1584, 1991.
33. **Neely JD, Christensen BM, Nielsen S, and Agre P.** Heterotetrameric composition of aquaporin-4 water channels. *Biochem J* 38: 11156–11163, 1999.
34. **Scheffers MS, Le H, van der BP, Leonhard W, Prins F, Spruit L, Breuning MH, De Heer E, and Peters DJ.** Distinct subcellular expression of endogenous polycystin-2 in the plasma membrane and Golgi apparatus of MDCK cells. *Hum Mol Genet* 11: 59–67, 2002.
35. **Schnermann J, Chou CL, Ma T, Traynor T, Knepper MA, and Verkman AS.** Defective proximal tubular fluid reabsorption in transgenic aquaporin-1 null mice. *Proc Natl Acad Sci USA* 95: 9660–9664, 1998.
36. **Sui H, Han BG, Lee JK, Walian P, and Jap BK.** Structural basis of water-specific transport through the AQP1 water channel. *Nature* 414: 872–878, 2001.
37. **Terris J, Ecelbarger CA, Marples D, Knepper MA, and Nielsen S.** Distribution of aquaporin-4 water channel expression within rat kidney. *Am J Physiol Renal Physiol* 269: F775–F785, 1995.
38. **Van Balkom BWM, Savelkoul PJ, Markovich D, Hofman E, Nielsen S, van der Sluijs P, and Deen PMT.** The role of putative phosphorylation sites in the targeting and shuttling of the aquaporin-2 water channel. *J Biol Chem* 277: 41473–41479, 2002.
39. **Van Balkom BWM, Van Raak M, Breton S, Pastor-Soler N, Bouley R, van der Sluijs P, Brown D, and Deen PMT.** Hypertonicity is involved in redirecting the aquaporin-2 water channel into the basolateral, instead of the apical, plasma membrane of renal epithelial cells. *J Biol Chem* 278: 1101–1107, 2003.
40. **van Os CH, Deen PMT, and Dempster JA.** Aquaporins: water selective channels in biological membranes. Molecular structure and tissue distribution. *Biochim Biophys Acta* 1197: 291–309, 1994.
41. **Walz T, Smith BL, Agre P, and Engel A.** The three-dimensional structure of human erythrocyte aquaporin CHIP. *EMBO J* 13: 2985–2993, 1994.